AIP Advances

Enhanced terahertz radiation of photoconductive antenna fabricated on GaAs-on-sapphire

Cite as: AIP Advances **9**, 125234 (2019); https://doi.org/10.1063/1.5127877
Submitted: 11 November 2019 . Accepted: 12 December 2019 . Published Online: 23 December 2019

Jitao Zhang, Mingguang Tuo, Michael Gehl, Ricky Gibson, Min Liang, and Hao Xin

Enhanced terahertz radiation of photoconductive antenna fabricated on GaAs-on-sapphire

Cite as: AIP Advances 9, 125234 (2019); doi: 10.1063/1.5127877
Submitted: 11 November 2019 • Accepted: 12 December 2019 •
Published Online: 23 December 2019

Jitao Zhang,[1,2,a] Mingguang Tuo,[1] Michael Gehl,[3] Ricky Gibson,[4] Min Liang,[1] and Hao Xin[1,a]

AFFILIATIONS

[1]Department of Electrical and Computer Engineering, The University of Arizona, Tucson, Arizona 85721, USA
[2]Fischell Department of Bioengineering, University of Maryland, College Park, Maryland 20742, USA
[3]Photonic and Phononic Microsystems, Sandia National Laboratory, Albuquerque, New Mexico 87123, USA
[4]Wyant College of Optical Sciences, The University of Arizona, Tucson, Arizona 85721, USA

[a]**Authors to whom correspondence should be addressed:** jtzhang4@umd.edu and hxin@ece.arizona.edu

ABSTRACT

The terahertz (THz) radiation properties of a photoconductive antenna (PCA) fabricated on a GaAs-on-sapphire (GoS) substrate are reported at sub-THz band. The GaAs layer with a thickness of approximately 1 μm was directly deposited on a sapphire wafer by means of molecular beam epitaxy. A butterfly-shaped antenna structure was then fabricated on the GoS substrate by photolithography, and the device was tested as the emitter of an in-house built THz time-domain spectrometer. The performance of this antenna was compared with a commercial one, which had an identical antenna structure but was fabricated on low-temperature-grown GaAs (LT-GaAs). The results showed that the GoS-based PCA radiated an enhanced THz field, which could be as much as 1.9 times that of the LT-GaAs-based PCA, indicating that GoS could be a promising photoconductive material. In addition, the optical transparency of the sapphire substrate allows the device to be illuminated from the backside, which is crucial for THz near-field imaging applications where the sample is usually in close proximity to the front surface of the PCA device.

Since its appearance in the 1980s, photoconductive antennas (PCAs) have been widely used as pulsed terahertz (THz) sources.[1–3] A PCA usually consists of a substrate, a metallic structure that is fabricated on top and an active layer in between. The THz radiation originates from the transient current within the PCA when its gap is excited by an ultrafast laser pulse. In the site where the photoexcited current is generated, the active layer is crucial for the THz radiation of the PCA. Generally speaking, the desired material of an active layer should have high optical-absorption, large dark conductivity, and short carrier lifetime so that the transient photoexcited current can be generated efficiently and then radiated out in the THz band. Along with the invention of the PCA, numerous materials have been demonstrated as the active layer, such as radiation-damaged silicon on sapphire (RD-SoS), InP, InGaAs, ion-implanted GaAs, semi-insulating GaAs, and low-temperature grown GaAs (LT-GaAs).[4–10] Among them, LT-GaAs is most frequently used in practice due to both high mobility and subpicosecond carrier lifetime.[11] The LT-GaAs layer is usually grown on a GaAs substrate with temperature around 250 °C by molecular beam epitaxy (MBE) equipment. However, regarding the applications where backside laser illumination (the laser beam transmits through the substrate before it illuminates the active layer) is required,[12,13] LT-GaAs substrates cannot be utilized because GaAs is opaque at the excitation laser wavelength. In order to make use of the advantages of LT-GaAs in such applications, Heiliger *et al.* has demonstrated the transfer of the LT-GaAs layer to a sapphire substrate, which is optically transparent (around 85% of transmission at 800 nm), using an epitaxial liftoff technique.[14] This makes the fabrication procedure more complicated and inefficient. In this letter, instead of layer transfer, the GaAs layer was directly grown on the sapphire substrate using MBE equipment. The THz radiation properties of the PCA fabricated on this GaAs-on-sapphire (GoS) substrate were evaluated by THz time-domain spectroscopy (THz-TDS). As a comparison, a commercial PCA with identical structure but fabricated on LT-GaAs was tested under the same conditions. The results show that the GoS-based PCA can radiate an enhanced THz

field compared to the LT-GaAs based PCA within the experimental conditions.

The schematics of the THz time-domain spectrometer and the cross section of two substrates illustrating the detailed layered structures are shown in Fig. 1. The polycrystalline GaAs layer was deposited on a sapphire wafer (C- to M-plane off by 0.2°, double-side polished, and a thickness of 430 μm) with the rate of 0.283 nm/s at 600 °C by the MBE equipment, and its ultimate thickness was approximately 1 μm. The MBE equipment is a research system (Riber 32) capable of depositing on a single 2-in. wafer. The as-grown GaAs layer has an rms surface roughness of 64 nm, which was measured by atomic force microscopy. The butterfly-shaped metallic structure was then fabricated on the top of the GoS wafer by a standard photolithography process. The central region of the structure is a coplanar stripline with a gap of 34 μm and a length of 100 μm. The width of the electrode is 5 μm. The metallic structure has a layered structure of 40-nm Cr/200-nm Au. As the last step, a 130-nm thick SiO_2 passivation layer was deposited on the top of the PCA to improve the optical transmission. A commercial PCA (model: PCA-44-34-100-800-h, BATOP GmbH) with an identical structure was taken as a comparison. It was fabricated on a 625-μm thick SI-GaAs substrate with a 3-μm LT-GaAs epilayer on top, and a SiO_2 passivation layer was also deposited. The chip size of the two PCAs is about 2 × 2 mm^2. The chip was then mounted onto the center of a 12-mm diameter hyperhemispherical silicon lens to help couple the THz field into free space.[15] An in-house built THz-TDS setup was used for the testing, as shown in Fig. 1(a). A Ti:sapphire femtosecond laser (Micra 5, Coherent, Inc.) with a center wavelength of 800 nm and a repetition rate of 80 MHz was used as the light source. The maximum output power of the laser was 400 mW, and the pulse width was 45 fs. The PCAs under study were used as THz emitters, and a commercial butterfly-shaped PCA (model: PCA-44-06-10-800-h, BATOP GmbH) with 6-μm gap dipole structure in the central region was used as the THz detector. The photoconductive current of the detector was measured by a lock-in amplifier (SR850, Stanford Research Systems). An optical chopper was used to modulate the laser beam and to provide a reference signal for the lock-in amplifier. The laser beam was fully focused on the gap region of the PCA. During testing, the PCA detector was illuminated by a 5 mW laser beam, and the PCAs under study were driven by various laser powers and DC bias voltages.

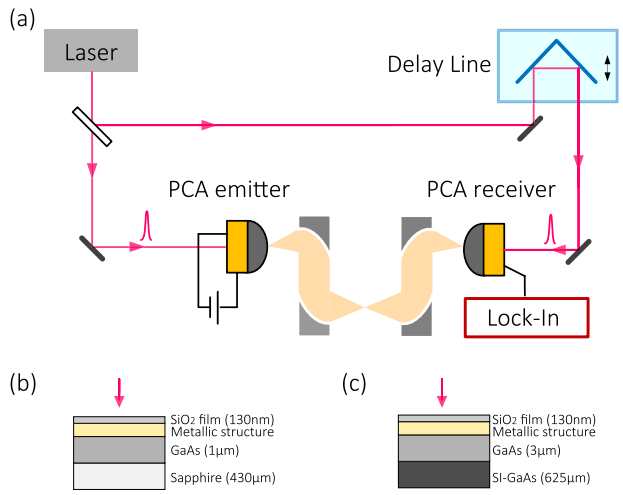

FIG. 1. Schematics of (a) THz time-domain spectrometer in transmission configuration, (b) GaAs-on-sapphire cross section, and (c) LT-GaAs cross section. The arrow in (b) and (c) indicates the illumination direction of the laser beam.

Figure 2 shows the time-domain THz pulses of the two PCAs and their corresponding spectra at 6 mW average laser power and 5 V bias voltage. It shows that the THz pulse (peak-to-peak value) of the GoS-based PCA is approximately 1.8 times that of the LT-GaAs-based PCA. In the frequency domain, a similar enhancement factor can be observed at the peak frequency (<0.1 THz). Since the butterfly-shaped PCA mainly works at a lower THz frequency band due to its large size of the metallic structure, we did not observe a distinct difference between both PCAs regarding the bandwidth.[16] For a comprehensive comparison, the illuminated laser power was swept from low to high powers at different bias voltages (i.e., 3 V, 7 V, 9 V, and 11 V) and the results are shown in Fig. 3. The relationship between the time-domain pulse (peak-to-peak) and the laser power was well fit with the scaling rule,[7,17] as shown in Eq. (1a). E_{THz} is the THz field, E_b is the bias field,P is the laser power, and D as well as P_0 has the form shown in Eqs. (1b) and (1c), respectively. A is the area of gap region, n is the refractive index of the substrate, ε_0 is the permittivity of free space, c is the speed of light in vacuum, η_0 is the impedance of free space, τ_d is the response time of the detector, z is the distance from the PCA emitter to PCA detector, h is Planck's constant, ν is the laser's frequency, e is the elementary charge, R is the reflectivity of the PCA surface, and μ is the electron's mobility,

$$E_{THz} \approx DE_b \frac{P}{P_0 + P}, \tag{1a}$$

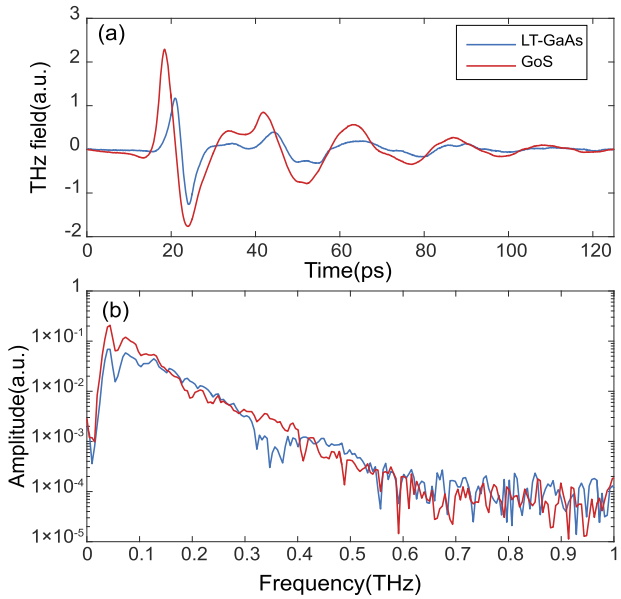

FIG. 2. (a) Time-domain THz pulses of the GoS-based PCA (red solid curve) and LT-GaAs-based PCA (blue solid curve) at 6 mW average laser power and 5 V bias voltage. (b) Corresponding spectra of the time-domain signals in (a) by fast Fourier transformation.

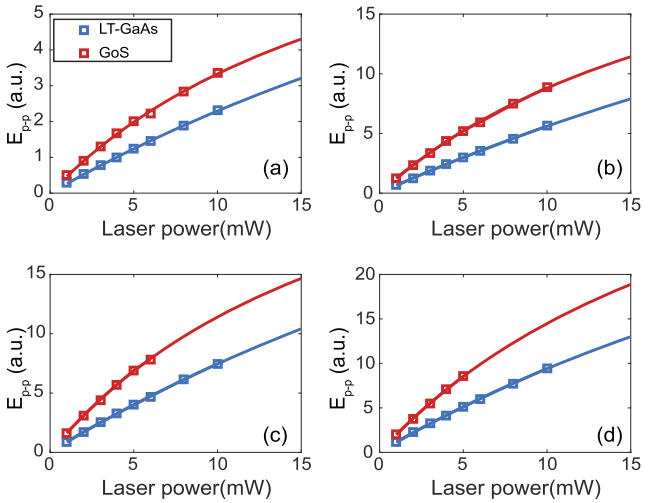

FIG. 3. THz field strength (peak-to-peak) as a function of the laser power at the bias voltage of (a) 3 V, (b) 7 V, (c) 9 V, and (d) 11 V. The solid curves were fit according to the scaling rule.

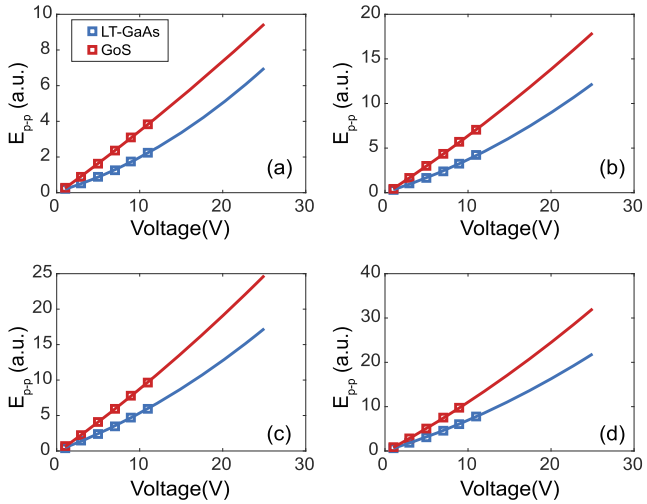

FIG. 5. THz field strength (peak-to-peak) with regard to the bias voltage at laser powers of (a) 2 mW, (b) 4 mW, (c) 6 mW, and (d) 8 mW. The solid curves were fit by quadratic curves.

$$D = \frac{A\sqrt{n}}{4\pi\varepsilon_0 c^2 \eta_0 \tau_d z}, \tag{1b}$$

$$P_0 = \frac{(1+n)h\nu}{e(1-R)\mu\eta_0}. \tag{1c}$$

D and P_0 were fit to the experimental data. The good agreement between experimental data and the fit line suggests that both PCAs follow the scaling rule. Figure 4 shows the corresponding enhancement at various conditions. The maximum enhancement of the THz field is 1.9, which was measured at 2 mW laser power and 7 V bias voltage. The fit curves predict that the GoS-based PCA still outperforms the LT-GaAs-based PCA as the laser power further increases. However, the enhancement ratio in Fig. 4 shows a monotonic decrease, which is probably due to the screening effect of the radiation field.

Moreover, the bias voltage was swept at different laser powers (i.e., 2 mW, 4 mW, 6 mW, and 8 mW) and the results are shown in Figs. 5 and 6. The experimental data in Fig. 5 did not show a good linear relationship as predicted by the scaling rule. Instead, it was fit better by a quadratic curve. The main reason

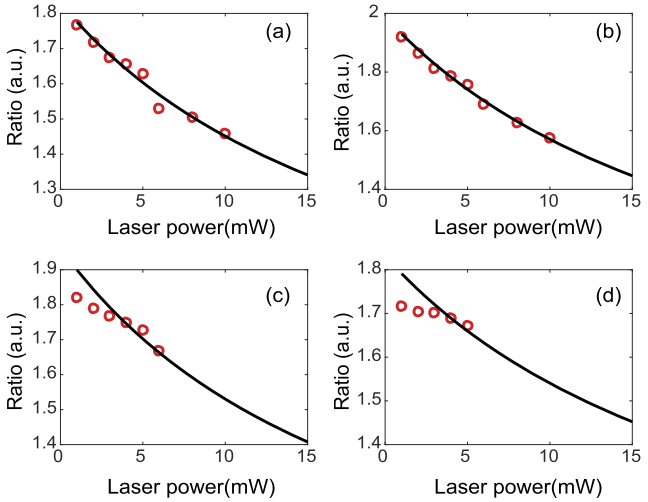

FIG. 4. Corresponding THz field enhancement ratio of the GoS-based PCA and the LT-GaAs-based PCA shown in Fig. 3 at (a) 3 V, (b) 7 V, (c) 9 V, and (d) 11 V. The open circle and solid line were the ratio of experimental data and fits to the data, respectively.

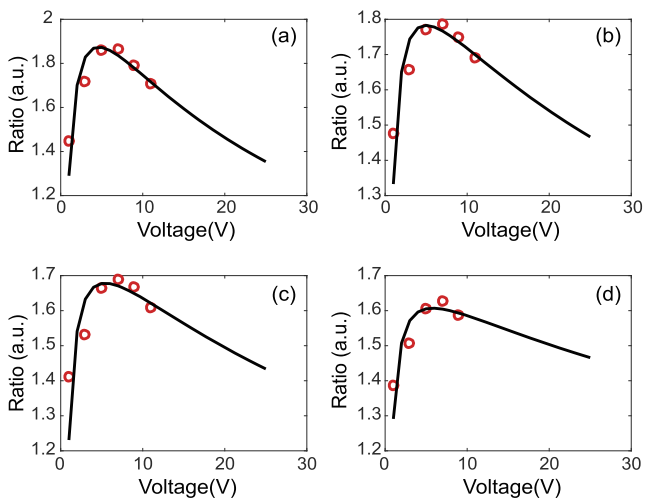

FIG. 6. Corresponding THz field enhancement ratio of the GoS-based PCA and the LT-GaAs-based PCA shown in Fig. 5 at (a) 2 mW, (b) 4 mW, (c) 6 mW, and (d) 8 mW. The open circle and solid line were the ratio of experimental data and fits to the data, respectively.

is probably due to the carrier mobility. In the model of scaling rule, the carrier mobility is assumed as constant. While in reality, it is strongly field-dependent, owing to the saturation velocity of the carriers in the semiconductor.[18] The enhancement ratio in Fig. 6 shows a nonmonotonic trend, which can be understood as the overall effect of both the free-space charge screening[19,20] and the field-dependent carrier mobility. The screening effect was predominant at very low bias for both PCAs, and the GoS-based PCA suffered less severe screening because of larger mobility. Therefore, the enhancement ratio was small at low bias voltages. However, with increasing bias field, the screening effect of free-space charges becomes weaker; thus, the ratio increases, which results in the rising part of the ratio curve. The peak of the ratio curve suggests that the screening effect from free-space charges becomes less important at higher bias voltages while the field-dependent mobility begins to dominate.

According to the scaling rule, the enhancement of the GoS-based PCA is mainly due to the larger mobility of carriers in the GaAs layer on sapphire relative to that of the LT-GaAs layer on SI-GaAs. The fit result shows that the mobility of GoS is about 3.08 times that of LT-GaAs. In experiment, the measured average photocurrent of GoS is 4.54 times that of LT-GaAs, which agrees with the prediction of the scaling rule. In addition, the dark resistance of the GoS-based PCA is 3.5 times that of the LT-GaAs-based PCA, which also suggests a higher mobility of carriers in the GoS substrate. As the mobility of the LT-GaAs is reported to be about 200–400 cm^2/V s,[21,22] we expect that the mobility of the GoS is around 600–1200 cm^2/V s. The increased mobility in GoS could be a result of multiple factors, such as the growth temperature and the polycrystalline structure of the GaAs layer. The carrier lifetime of GaAs layers depends on both the growth temperature and crystal structure. While GaAs grown at low temperatures (<300 °C) usually has carrier lifetimes of less than 1 ps, we expect that the GaAs layer on sapphire may still have short carrier lifetime due to its polycrystalline structure. In our experiments, limited by the radiation bandwidth of the metallic structure, we did not observe a distinct difference between two PCAs regarding the THz bandwidth. In the future, PCAs with different structures (such as dipole, stripline, or bowtie) can be fabricated to study the performance of GoS in the broad THz band.

In summary, a photoconductive material was grown by directly depositing GaAs on a sapphire wafer. The THz emission properties of the PCA fabricated on this GoS substrate were reported. Enhanced THz radiation was observed in comparison to an identical antenna structure fabricated on LT-GaAs, which is mainly attributed to the larger mobility of the GoS, a factor closely related to the growth temperature and crystal structure. A further understanding of this active layer could be achieved by comparing it with the transferred GaAs layer on the same substrate via the liftoff technique. This work indicates that, as an alternative to LT-GaAs on SI-GaAs wafers, GoS could be a promising photoconductive material.

This work was financially supported by the National Science Foundation Major Research Instrument Program (Grant No. 1126572), Air Force Office of Scientific Research (AFOSR, Dr. Gernot Pomrenke, Grant No. FA9550-12-1-0003), and NSF-ERC Center for Integrated Access Networks (CIAN). We would like to thank Dr. Galina Khitrova for providing supervision of the material growth. This paper describes objective technical results and analysis. Any subjective views or opinions that might be expressed in the paper do not necessarily represent the views of the U.S. Department of Energy or the United States Government.

REFERENCES

[1] D. Auston, K. Cheung, and P. Smith, Appl. Phys. Lett. **45**, 284 (1984).
[2] N. M. Burford and M. O. El-Shenawee, Opt. Eng. **56**, 010901 (2017).
[3] E. Castro-Camus and M. Alfaro, Photonics Res. **4**, A36 (2016).
[4] M. Ketchen, D. Grischkowsky, T. Chen, C. C. Chi, I. Duling III, N. Halas, J. M. Halbout, J. Kash, and G. Li, Appl. Phys. Lett. **48**, 751 (1986).
[5] B. Salem, D. Morris, V. Aimez, J. Beerens, J. Beauvais, and D. Houde, J. Phys.: Condens. Matter **17**, 7327 (2005).
[6] M. Tani, S. Matsuura, K. Sakai, and S.-i. Nakashima, Appl. Opt. **36**, 7853 (1997).
[7] P. Benicewicz, J. Roberts, and A. Taylor, J. Opt. Soc. Am. B **11**, 2533 (1994).
[8] A. Krotkus, J. Phys. D: Appl. Phys. **43**, 273001 (2010).
[9] R. Kohlhaas, S. Breuer, S. Nellen, L. Liebermeister, M. Schell, M. Semtsiv, W. Masselink, and B. Globisch, Appl. Phys. Lett. **114**, 221103 (2019).
[10] E. A. P. Prieto, S. A. B. Vizcara, L. P. Lopez, J. D. E. Vasquez, M. H. M. Balgos, D. Hashizume, N. Hayazawa, Y. Kim, M. Tani, and A. S. Somintac, Opt. Mater. Express **8**, 1463 (2018).
[11] M. C. Beard, G. M. Turner, and C. A. Schmuttenmaer, J. Appl. Phys. **90**, 5915 (2001).
[12] O. Mitrofanov, I. Brener, R. Harel, J. Wynn, L. Pfeiffer, K. West, and J. Federici, Appl. Phys. Lett. **77**, 3496 (2000).
[13] A. Bitzer, A. Ortner, and M. Walther, Appl. Opt. **49**, E1 (2010).
[14] H. M. Heiliger, M. Vossebürger, H. Roskos, H. Kurz, R. Hey, and K. Ploog, Appl. Phys. Lett. **69**, 2903 (1996).
[15] J. Van Rudd and D. M. Mittleman, J. Opt. Soc. Am. B **19**, 319 (2002).
[16] J. Zhang, M. Tuo, M. Liang, X. Wang, and H. Xin, J. Appl. Phys. **124**, 053107 (2018).
[17] P. Benicewicz and A. Taylor, Opt. Lett. **18**, 1332 (1993).
[18] D. Caughey and R. Thomas, Proc. IEEE **55**, 2192 (1967).
[19] D. S. Kim and D. Citrin, Appl. Phys. Lett. **88**, 161117 (2006).
[20] G. C. Loata, M. D. Thomson, T. Löffler, and H. G. Roskos, Appl. Phys. Lett. **91**, 232506 (2007).
[21] D. C. Look, Thin Solid Films **231**, 61 (1993).
[22] G. Segschneider, F. Jacob, T. Löffler, H. G. Roskos, S. Tautz, P. Kiesel, and G. Döhler, Phys. Rev. B **65**, 125205 (2002).